

# Charged particle reconstruction for future high energy colliders with Quantum Approximate Optimization Algorithm

Hideki Okawa<sup>[0000-0002-2548-6567]</sup>

Institute of High Energy Physics, Chinese Academy of Sciences, Shijingshan Beijing 100049, China [okawa@ihep.ac.cn](mailto:okawa@ihep.ac.cn)

**Abstract.** Usage of cutting-edge artificial intelligence will be the baseline at future high energy colliders such as the High-Luminosity Large Hadron Collider, to cope with the enormously increasing demand of the computing resources. The rapid development of quantum machine learning could bring in further paradigm-shifting improvement to this challenge. One of the two highest CPU-consuming components, the charged particle reconstruction, the so-called track reconstruction, can be considered as a quadratic unconstrained binary optimization (QUBO) problem. The Quantum Approximate Optimization Algorithm (QAOA) is one of the most promising algorithms to solve such combinatorial problems and to seek for a quantum advantage in the era of the Noisy Intermediate-Scale Quantum computers. It is found that the QAOA shows promising performance and demonstrated itself as one of the candidates for the track reconstruction using quantum computers.

**Keywords:** Quantum Machine Learning · QUBO · QAOA · High Energy Physics · track reconstruction

## 1 Introduction

High energy physics aims to unveil the laws of the fundamental building blocks of matter, the elementary particles, and their interactions. High energy colliders have been one of the most promising approaches to discover new particles and deepen understanding of the underlying physics through precise measurements. After the revolutionary discovery of the Higgs boson in 2012 [9,23] at the ATLAS [8] and CMS [22] experiments at the Large Hadron Collider (LHC) [25], we are entering the precision measurement era of the Higgs sector, first of all, to be pursued at the High-Luminosity LHC (HL-LHC) [34], and to be followed by future colliders being proposed, such as the Circular Electron Positron Collider (CEPC) [17,18,19,20] to be hosted in China.

At the HL-LHC, we will enter the “Exa-byte” era, where the annual computing cost will increase by a factor of 10 to 20. Without various innovations, the experiment will not be able to operate. Usage of the Graphical Processing Units (GPUs) and other state-of-the-art artificial intelligence (AI) technologies

such as deep learning will be the baseline at the HL-LHC. However, the emerging rapid development of quantum computing and implementation of machine learning techniques in such computers could bring in another leap. Two of the highly CPU consuming components at the LHC and HL-LHC are (1) the charged particle reconstruction, the so-called track reconstruction, for both in data and simulation and (2) simulation of electromagnetic and hadronic shower development in the calorimeter. Development of quantum machine learning techniques to overcome such challenges would not only be important for the HL-LHC, but also for a future Higgs factory CEPC and a next generation discovery machine the Super Proton-Proton Collider (SppC) [17,18] to be hosted in China as well as other such colliders under consideration in the world.

## 2 Track Reconstruction

Track reconstruction or tracking is the standard procedure in the collider experiments to identify charged particles traversing the detector and to measure their momenta. The curvature of particle trajectories (tracks) bent in a magnetic field will provide the momentum information. Tracks are reconstructed from hits in the silicon detectors, which have many irrelevant hits from secondary particles and detector noise, and require sophisticated algorithms. Tracking is one of the most crucial components of reconstruction in the collider experiments.

At the HL-LHC, additional proton-proton interactions per bunch crossing, the so-called pileup, becomes exceedingly high, and the CPU time required to run the track reconstruction explodes with pileup [10,21].

### 2.1 Current classical benchmarks

The Kalman Filter technique [30] has been often used as a standard algorithm to reconstruct the tracks. It is implemented in A Common Tracking Software (ACTS) [1], for example. Seeding from the inner detector layers, the tracks are extrapolated to predict the next hit and iterated to find the best quality combination. It is a well established procedure and has excellent performance but suffers from the computing time, especially when the track multiplicity per event becomes high.

Recently, usage of the graph neural network (GNN) is actively investigated at the LHC [35,37] as well as other collider experiment including the tau-lepton and charm-quark factory in China: Beijing Spectrometer (BES) III [14]. Hits in the silicon detectors can be regarded as “nodes” of the graphs, and segments reconstructed by connecting the hits can be considered as “edges”. GNN-based algorithms provide compatible performance as the Kalman Filter, but the computing time scales approximately linearly instead of exponentially with the number of tracks. The GNN is thus considered to be one of the new standards in the era of the HL-LHC.

## 2.2 Quantum approach

There have been several studies to run the track reconstruction with quantum computers. First of all, doublets are formed by connecting two hits in the silicon detectors. Then, triplets, segments with three silicon hits, are formed by connecting the doublets. Then, triplets are connected to reconstruct the tracks, by evaluating the consistency of the triplet momenta. Such procedure can be considered as a quadratic unconstrained binary optimization (QUBO) problem:

$$O(a, b, T) = \sum_{i=1}^N a_i T_i + \sum_{i=1}^N \sum_{j<i}^N b_{ij} T_i T_j, \quad (1)$$

where  $N$  is the number of triplets,  $T_i$  and  $T_j$  corresponds to the triplets and takes the value of either zero or one,  $a_i$  are the bias weights to evaluate the quality of the triplets, and  $b_{ij}$  are the coefficients that quantify the compatibility of two triplets ( $b_{ij} = 0$  if no shared hit,  $= 1$  if there is any conflict, and  $= -S_{ij}$  if two hits are shared between the triplets). The coefficients  $-S_{ij}$  quantify the consistency of the two triplet momenta by [12]:

$$S_{ij} = \frac{1 - \frac{1}{2}(|\delta(q/p_{T_i}, q/p_{T_j})| + \max(\delta\theta_i, \delta\theta_j))}{(1 + H_i + H_j)^2}, \quad (2)$$

where  $\delta$  is the difference between the curvature  $q/p_T$  or angle  $\theta$  of the two triplets and  $H_i$  is the number of holes in the triplet.

The bias weights  $a_i$  have significant impact on the Hamiltonian energy landscape and thus on the track reconstruction and computation speed. They can be parameterized as:

$$a_i = \alpha \left(1 - e^{-\frac{|d_0|}{\gamma}}\right) + \beta \left(1 - e^{-\frac{|z_0|}{\lambda}}\right), \quad (3)$$

where  $d_0$  and  $z_0$  are the transverse and longitudinal displacements of the triplets from the primary vertex (the most significant proton-proton collision point in an event) and  $\alpha$ ,  $\beta$ ,  $\gamma$  and  $\lambda$  are tunable parameters, which are taken to be 0.5, 0.2, 1.0 and 0.5, optimized in a previous study [39] for the same dataset (see Section 3).

The first quantum tracking studies [12,47] have been pursued with quantum annealing computers. The quantum annealer looks for the global minimum of a given function with quantum tunneling. It is a natural machine to solve QUBO problems by searching for the ground state of a Hamiltonian. As the size of the QUBO generally exceeds the number of available qubits in the current era of the Noisy Intermediate-Scale Quantum (NISQ) computers [42], the QUBO is split into subsets (sub-QUBOs) to search for the ground state. Performance evaluation between the D-Wave annealing machine and a classical emulation using a digital annealer is mentioned in Ref. [43]. The performance dependence against the size of the sub-QUBOs is evaluated in Ref. [44].

To exploit the quantum gate computers, a QUBO can be mapped to an Ising Hamiltonian and be solved using the Variational Quantum Eigensolver (VQE),

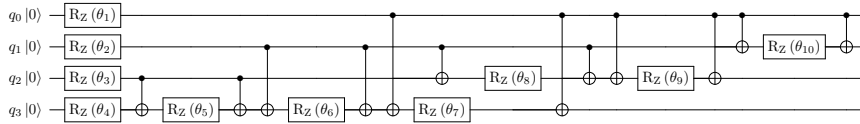


Fig. 1: Layout of the QAOA with the Quantum Alternative Operator Ansatz. The number of qubits is reduced to four for the demonstration purpose.

Quantum Approximate Optimization Algorithm (QAOA) [28], or other similar algorithms. Previous studies conducted at the LUXE experiment considered the TwoLocal ansatz with the  $R_Y$  gates and a circular CNOT entangling pattern [31,24]. The LHCb Collaboration has also looked into the QUBO approach with the gate computer using the Harrow-Hassadim-Lloyd (HHL) algorithm [40].

Another distinctive approach is pursued with the hybrid quantum classical GNN, where some components of the classical GNN method [35,37] are replaced by the Variational Quantum Layers. This hybrid model performs similarly to the classical approach, as also confirmed by Refs. [31,24]. This hybrid quantum-classical GNN approach is out of the scope of this paper, and will not be mentioned further.

### 3 Datasets

In this study, the dataset from the TrackML Challenge is adopted [6,7]. It is an open source dataset representing the conditions for the ATLAS and CMS experiments at the HL-LHC. It assumes the particle multiplicities expected with the pileup condition of  $\langle\mu\rangle=200$ . The dataset is simplified by focusing on the barrel (central) region of the detector, thus removing the hits in the end-cap region, which is a common approach often adopted for tracking studies for the HL-LHC.

The QUBO matrix, namely the bias weights  $a_i$  and the compatibility coefficients  $b_{ij}$  as defined in Equation 1 is extracted from the dataset using the hepqr-qallase library [2]. The QUBO matrix is pretty sparse, as is the nature of the collider experiments and track reconstruction.

### 4 Methodology

The QAOA is considered in this study. It is a hybrid quantum-classical method, designed to solve combinatorial optimization problems. Even at the lowest circuit depth, the QAOA cannot efficiently be simulated by classical computers, but has non-trivial guarantees on the performance [28,29]. For cases where the minimum energy spectrum gap is very small, the computing time required in the quantum annealers is very long to remain adiabatic. The QAOA is known to outperform adiabatic quantum annealing by several orders of magnitude in such

circumstances [45]. Thus, the QAOA is one of the most promising algorithm to seek for quantum advantage in the era of the NISQ computers.

Its libraries are implemented in pyqpanda-algorithm [3] by Origin Quantum (Chinese name: Benyuan). It adopts the Quantum Alternative Operator Ansatz [32]. The schematic layout of the quantum circuit is demonstrated in Fig. 1. For the actual hardware computation, the 6-qubit machine Wuyuan is used through the cloud service [4].

#### 4.1 Optimization of QAOA implementation

To optimize the conditions to run the QAOA, a  $6 \times 6$  matrix is extracted from a TrackML QUBO to match the available number of qubits in Wuyuan. Performance is evaluated for two loss functions: CVaR [13] and Gibbs [38]; three optimizers which can handle bounds on the variables: L-BFGS-B [16,46], Sequential Least Squares Programming (SLSQP) [36], and a Truncated Newtonian algorithm (TNC) [16]; and the number of layers of the QAOA.

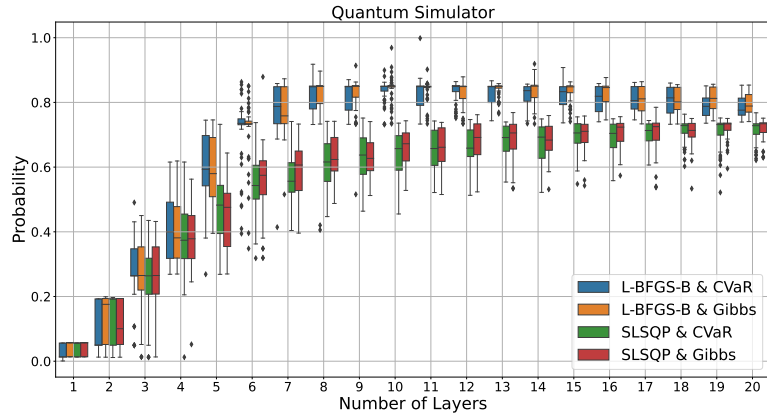
Fig. 2 shows the probability of finding the correct minimum energy with various loss functions, optimizers and the number of the QAOA layers for the quantum simulator and the actual quantum hardware. The probabilities tend to be low for the shallow QAOA, which is consistent with what is reported in Refs. [15,33,26,27]. Among the three optimizers, L-BFGS-B shows the best performance, followed by SLSQP. TNC shows largely degraded probabilities without much improvement against the number of layers, thus, is not presented in the figure. There is no significant difference between the CVaR and Gibbs loss functions, thus CVaR is adopted onward in this work. The real hardware shows compatible performance as the quantum simulator, and there is no sign of degradation even for deep-layer QAOAs up to 20 layers. This is in contrast to what is observed in Ref. [41] but consistent with Ref. [44]. This could be due to the difference in the QUBO considered, which is largely sparse in this paper as well as in Ref. [44].

It is worth emphasizing that in the actual implementation, a single QAOA job will run multiple shots and the combination with the highest probability will be selected. Thus, the accuracy of obtaining the correct answer is much higher than the probability itself, reaching 100% already at 5 layers as is presented in Fig. 3. In the following sections, seven QAOA layers are adopted, where the probability reaches the plateau and the accuracy is compatible with 100% within the statistical uncertainty.

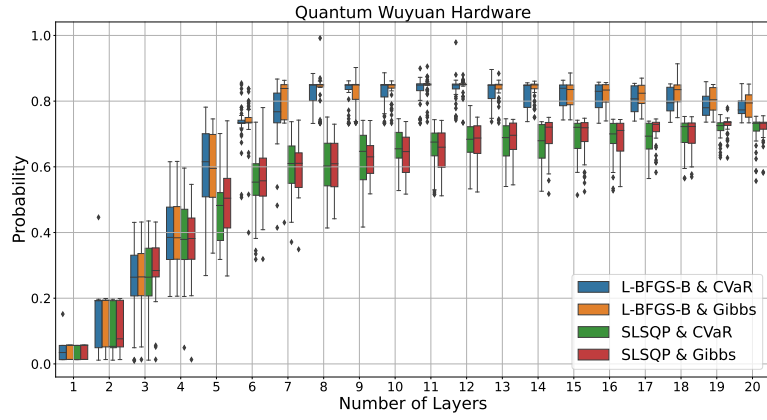
#### 4.2 Sub-QUBO method

The number of triplet candidates define the number of qubits required. Obviously the quantum computing resources currently available in the NISQ era cannot cover the full QUBO for tracking. Thus, the QUBO is split into sub-QUBOs of size  $6 \times 6$  to match the Wuyuan hardware.

There are various sub-QUBO algorithms proposed: qbsolv [5] (now in the dwave-hybrid library), for example. In this paper, a sub-QUBO method using



(a)



(b)

Fig. 2: Probability of finding the correct combination with the L-BFGS-B or SLSQP optimizers and the CVaR or Gibbs loss functions, presented against the number of QAOA layers for the quantum simulator (a) and Wuyuan hardware (b).

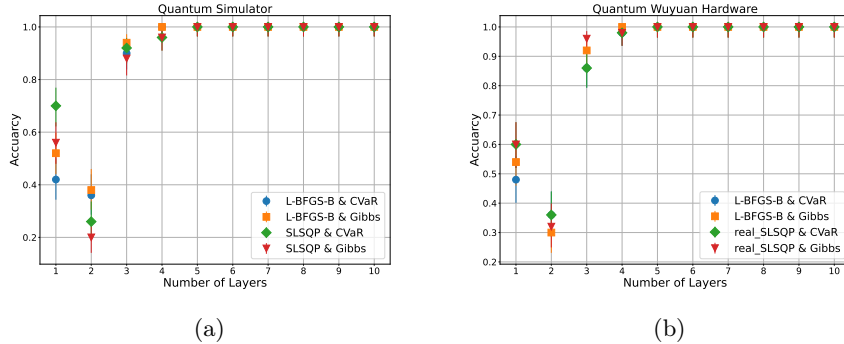


Fig. 3: Accuracy of finding the correct combination in a single job with the L-BFGS-B or SLSQP optimizers and the CVaR or Gibbs loss functions, presented against the number of QAOA layers for the quantum simulator (a) and real hardware (b). The statistical uncertainty is presented in the error bars.

multiple solution instances [11] is adopted. This method has a strong theoretical justification, whereas other existing approaches are heuristic and lack in such a foundation [11]. In this multiple solution instance method, three parameters ( $N_I$ ,  $N_E$ ,  $N_S$ ) are considered. First of all,  $N_I$  quasi-optimal solutions are extracted from the full-QUBO classically. Then  $N_S$  solution instances from  $N_I$  are randomly selected. The method focuses on a particular binary variable  $T_i$  (see Equation 1), rank them in accordance to how much they vary over  $N_S$  solution instances. Highly varying  $T_i$  will be included in the sub-QUBO model. The pick-up process of  $N_S$  solutions from the QAOA is repeated  $N_E$  times and  $N_E$  sub-QUBO models are considered. Finally, a pool of  $N_I$  solutions is returned and the best solution is chosen.

Fig. 4 shows the presumed minimum energy found by the multiple solution instance method for various sets of ( $N_I$ ,  $N_E$ ,  $N_S$ ) parameters with the quantum simulator compared to a simple classical optimizer with the simulated thermal annealing. Those two examples have the full QUBO size of  $778 \times 778$  and  $1431 \times 1431$  respectively, and correspond to the first two points later presented in Fig. 5 in Section 5. The output from the real quantum hardware Wuyuan is also presented for one set of the ( $N_I$ ,  $N_E$ ,  $N_S$ ) parameters. It is clearly observed that this sub-QUBO method using the QAOA succeeds in obtaining lower energy than the classical simulated annealing. There is no obvious dependence in performance on the three parameters. These two features of the method are consistent with what have been reported in the original proposal of this sub-QUBO method [11]. As the computing time increases with the size of the parameters, ( $N_I, N_E, N_S$ ) = (20, 10, 5) is adopted for the final evaluation on the tracking performance, which will be summarized in the next section. It is also promising to see that there is no degradation in performance with the actual quantum hardware despite the presence of noise.

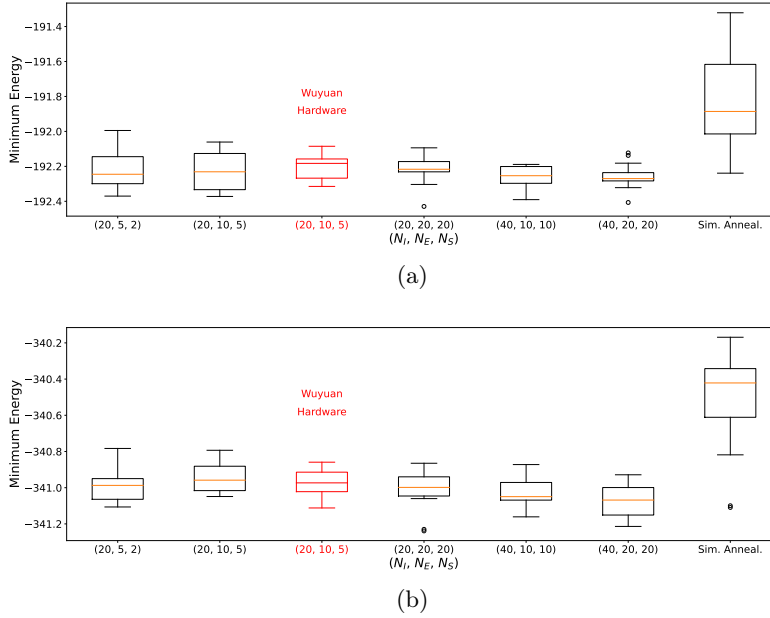


Fig. 4: Minimum energy estimated by the multiple solution instance method for various  $(N_I, N_E, N_S)$  parameters with the quantum simulator and Wuyuan hardware compared to a classical simulated thermal annealing. Two examples with the full QUBO size of  $778 \times 778$  (a) and  $1431 \times 1431$  (b) are presented.

## 5 Results and Discussions

Several events are selected containing a few thousands particles and noise. The track reconstruction is pursued by running the sub-QUBO method with the three parameters  $(N_I, N_E, N_S)$  defined in the previous section. The QAOA utilizes seven layers and the CVaR loss function, and split into sub-QUBOs with the size of six qubits.

Performance of the track reconstruction is evaluated in terms of efficiency (recall) and purity (precision). They are defined as the following:

$$\text{Efficiency} = \frac{TP}{TP + FN} = \frac{\# \text{ of matched reconstructed doublets}}{\# \text{ of true doublets}}, \quad (4)$$

$$\text{Purity} = \frac{TP}{TP + FP} = \frac{\# \text{ of matched reconstructed doublets}}{\# \text{ of all reconstructed doublets}}, \quad (5)$$

where  $TP$  is the true positives,  $FN$  the false negatives, and  $FP$  the false positives.  $TP$  corresponds to the number of reconstructed doublets matching to the correct (true) doublets.  $FN$  is the number of true doublets that are not reconstructed, thus  $TP + FN$  is simply the number of true doublets.  $FP$  is the



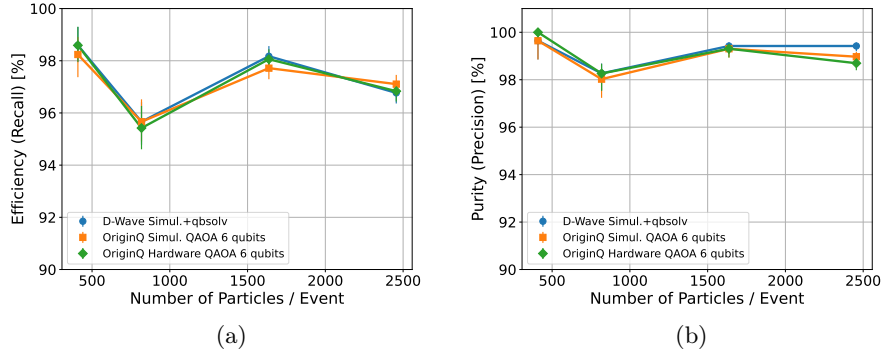


Fig. 5: Efficiency (a) and purity (b) as a function of particle multiplicity utilizing the QAOA simulator, Wuyuan hardware or the D-Wave simulator with qbsolv.

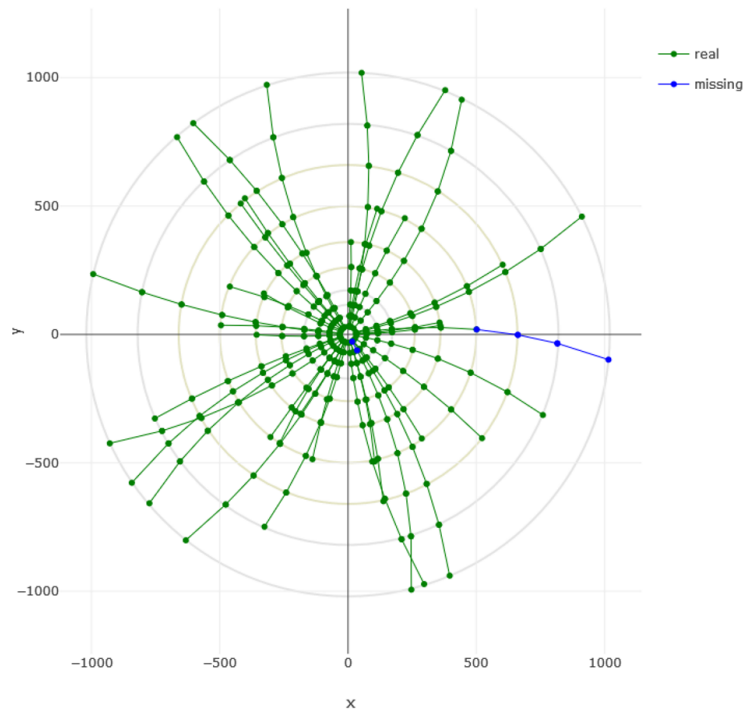
number of reconstructed doublets that do not match to the true doublets. In the high energy physics terminology, they are called the “fake” doublets.

Fig. 5 shows the track efficiency and purity using the QAOA with the quantum simulator or Wuyuan hardware. The performance is compared to the D-Wave simulator approach implemented in Ref. [12]. The D-Wave simulator with qbsolv and NEAL show almost indistinguishable results, so only the qbsolv values are shown in the figure. The track reconstruction performance with QAOA is compatible with the D-Wave annealing approach, and there is no sign of degradation in the actual hardware. Fig. 6 presents two event displays from the lowest and highest particle density events considered in Fig. 5.

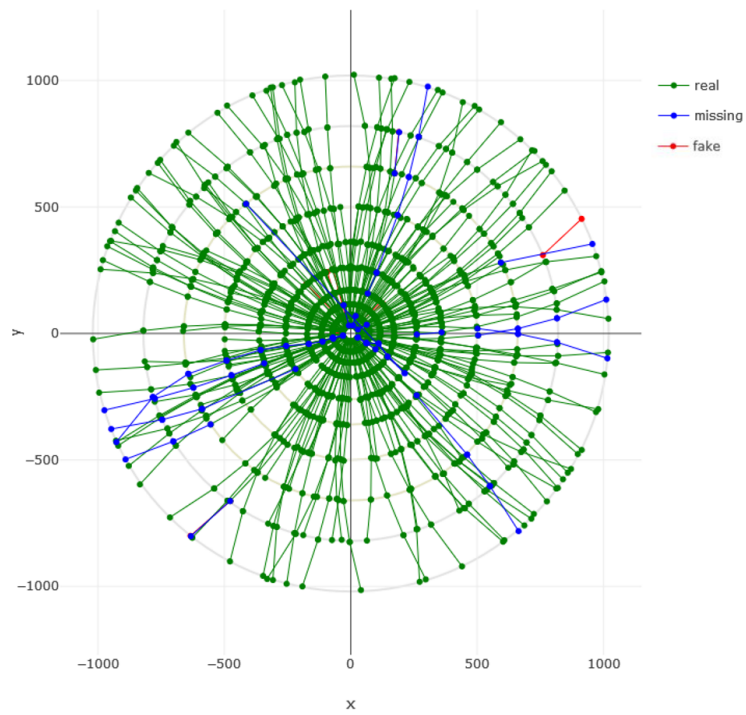
This work demonstrates that the QAOA is a promising candidate to be considered for the track reconstruction at the future colliders. With utilizing a robust sub-QUBO method and the QAOA, high performance can be achieved even with a small size of qubits. The compatible performance obtained with the real quantum hardware further supports its potential usability.

It is not yet at the stage to evaluate the quantum advantage, since the QAOA with six qubits can run quickly on the quantum simulator as well with compatible performance. The non-trivial impact is to be investigated with higher qubit conditions, which would be beyond the reach of the quantum simulator and is left for future studies.

**Acknowledgements** The author would like to thank Federico Meloni and David Spataro for discussions regarding the quantum tracking and Andreas Salzburger for his suggestion on the TrackML dataset. The author would also like to thank Ziwei Cui and Lei Li from Origin Quantum (Benyuan) for various feedback. The author is supported by NSFC under contract No. 12075060. This work is benefited by the libraries and quantum computing resources provided by Origin Quantum.



(a)



(b)

Fig. 6: Event displays of tracks reconstructed with the QAOA utilizing the Wuyuan hardware. They are generated with hepqr-qallase library [2].

## References

1. <https://acts.readthedocs.io/en/latest/>
2. <https://github.com/derlin/heppqr-qallse>
3. <https://pyqpanda-algorithm-tutorial.readthedocs.io/en/latest/>
4. <https://qcloud.originqc.com.cn/>
5. <https://docs.ocean.dwavesys.com/projects/qbsolv/en/latest/index.html>
6. Amrouche, S., et al.: The Tracking Machine Learning challenge : Accuracy phase. The NeurIPS '18 Competition: From Machine Learning to Intelligent Conversations, arXiv:1904.06778 (2019). [https://doi.org/10.1007/978-3-030-29135-8\\_9](https://doi.org/10.1007/978-3-030-29135-8_9)
7. Amrouche, S., et al.: The Tracking Machine Learning Challenge: Throughput Phase. *Comput. Softw. Big Sci.* **7**(1), 1 (2023). <https://doi.org/10.1007/s41781-023-00094-w>
8. ATLAS Collaboration: The ATLAS Experiment at the CERN Large Hadron Collider. *JINST* **3**, S08003 (2008). <https://doi.org/10.1088/1748-0221/3/08/S08003>
9. ATLAS Collaboration: Observation of a new particle in the search for the Standard Model Higgs boson with the ATLAS detector at the LHC. *Phys. Lett. B* **716**, 1–29 (2012). <https://doi.org/10.1016/j.physletb.2012.08.020>
10. ATLAS Collaboration: Fast Track Reconstruction for HL-LHC. ATL-PHYS-PUB-2019-041 (2019), <https://cds.cern.ch/record/2693670>
11. Atobe, Y., Tawada, M., Togawa, N.: Hybrid Annealing Method Based on subQUBO Model Extraction With Multiple Solution Instances. *IEEE Trans. Comp.* **71**(10), 2606 (2022)
12. Bapst, F., Bhimji, W., Calafiura, P., Gray, H., Lavrijsen, W., Linder, L.: A pattern recognition algorithm for quantum annealers. *Comput. Softw. Big Sci.* **4**(1), 1 (2020). <https://doi.org/10.1007/s41781-019-0032-5>
13. Barkoutsos, P.K., Nannicini, G., Robert, A., Tavernelli, I., Woerner, S.: Improving Variational Quantum Optimization using CVaR. *Quantum* **4**, 256 (2020). <https://doi.org/10.22331/q-2020-04-20-256>
14. BES III Collaboration: Design and Construction of the BESIII Detector. *Nucl. Instrum. Meth. A* **614**, 345–399 (2010). <https://doi.org/10.1016/j.nima.2009.12.050>
15. Bravyi, S., Kliesch, A., Koenig, R., Tang, E.: Obstacles to variational quantum optimization from symmetry protection. *Phys. Rev. Lett.* **125**, 260505 (2020). <https://doi.org/10.1103/PhysRevLett.125.260505>
16. Byrd, R.H., Lu, P., Nocedal, J., Zhu, C.: A limited memory algorithm for bound constrained optimization. *SIAM Journal on Scientific Computing* **16**(5), 1190–1208 (1995)
17. CEPC-SPPC Study Group: CEPC-SPPC Preliminary Conceptual Design Report. 1. Physics and Detector. IHEP-CEPC-DR-2015-01, IHEP-TH-2015-01, IHEP-EP-2015-01 (2015)
18. CEPC-SPPC Study Group: CEPC-SPPC Preliminary Conceptual Design Report. 2. Accelerator. IHEP-CEPC-DR-2015-01, IHEP-AC-2015-01 (2015)
19. CEPC Study Group: CEPC Conceptual Design Report: Volume 1 - Accelerator. IHEP-CEPC-DR-2018-01, IHEP-AC-2018-01 (2018)
20. CEPC Study Group: CEPC Conceptual Design Report: Volume 2 - Physics & Detector. IHEP-CEPC-DR-2018-02, IHEP-EP-2018-01, IHEP-TH-2018-01 (2018)

21. Cerati, G.B.: Tracking and vertexing algorithms at high pileup. Conference Report CMS-CR-2014-345 (2014), <https://cds.cern.ch/record/1966040>
22. CMS Collaboration: The CMS Experiment at the CERN LHC. JINST **3**, S08004 (2008). <https://doi.org/10.1088/1748-0221/3/08/S08004>
23. CMS Collaboration: Observation of a New Boson at a Mass of 125 GeV with the CMS Experiment at the LHC. Phys. Lett. B **716**, 30–61 (2012). <https://doi.org/10.1016/j.physletb.2012.08.021>
24. Crippa, A., et al.: Quantum algorithms for charged particle track reconstruction in the LUXE experiment. DESY-23-045, MIT-CTP/5481, arXiv:2304.01690 (2023)
25. Evans, L., Bryant, P.: LHC Machine. JINST **3**, S08001 (2008). <https://doi.org/10.1088/1748-0221/3/08/S08001>
26. Farhi, E., Gamarnik, D., Gutmann, S.: The quantum approximate optimization algorithm needs to see the whole graph: A typical case. arXiv:2004.09002 (2020)
27. Farhi, E., Gamarnik, D., Gutmann, S.: The quantum approximate optimization algorithm needs to see the whole graph: Worst case examples. arXiv:2005.08747 (2020)
28. Farhi, E., Goldstone, J., Gutmann, S.: A quantum approximate optimization algorithm. arXiv:1411.4028 (2014)
29. Farhi, E., Goldstone, J., Gutmann, S.: A quantum approximate optimization algorithm applied to a bounded occurrence constraint problem. arXiv:1412.6062 (2015)
30. Fruhwirth, R.: Application of Kalman filtering to track and vertex fitting. Nucl. Instrum. Meth. A **262**, 444–450 (1987). [https://doi.org/10.1016/0168-9002\(87\)90887-4](https://doi.org/10.1016/0168-9002(87)90887-4)
31. Funcke, L., Hartung, T., Heinemann, B., Jansen, K., Kropf, A., Kühn, S., Meloni, F., Spataro, D., Tüysüz, C., Yap, Y.C.: Studying quantum algorithms for particle track reconstruction in the LUXE experiment. J. Phys. Conf. Ser. **2438**(1), 012127 (2023). <https://doi.org/10.1088/1742-6596/2438/1/012127>
32. Hadfield, S., Wang, Z., O’Gorman, B., Rieffel, E.G., Venturelli, D., Biswas, R.: From the quantum approximate optimization algorithm to a quantum alternating operator ansatz. Algorithms **12**(2) (2019). <https://doi.org/10.3390/a12020034>
33. Hastings, M.B.: Classical and quantum bounded depth approximation algorithms. arXiv:1905.07047 (2019)
34. I. Béjar Alonso, O. Brüning, P. Fessia, M. Lamont, L. Rossi, L. Tavian, M. Zerlauth (editors): High-Luminosity Large Hadron Collider (HL-LHC): Technical design report. CERN Yellow Reports: Monographs, CERN, Geneva (2020). <https://doi.org/10.23731/CYRM-2020-0010>, <https://cds.cern.ch/record/2749422>
35. Ju, X., et al.: Graph Neural Networks for Particle Reconstruction in High Energy Physics detectors. In: 33rd Annual Conference on Neural Information Processing Systems (2020)
36. Kraft, D.: A software package for sequential quadratic programming. Tech. Rep. DFVLR-FB, 88-28, DLR German Aerospace Center – Institute for Flight Mechanics, Köln, Germany (1988)
37. Lazar, A., et al.: Accelerating the Inference of the Exa.TrkX Pipeline. J. Phys. Conf. Ser. **2438**(1), 012008 (2023). <https://doi.org/10.1088/1742-6596/2438/1/012008>
38. Li, L., Fan, M., Coram, M., Riley, P., Leichenauer, S.: Quantum optimization with a novel gibbs objective function and ansatz architecture search. Phys. Rev. Res. **2**, 023074 (2020). <https://doi.org/10.1103/PhysRevResearch.2.023074>
39. Linder, L.: Using a Quantum Annealer for particle tracking at LHC, Master Thesis at EPFL (2019)

40. Nicotra, D., Lucio Martinez, M., de Vries, J.A., Merk, M., Driessens, K., Westra, R.L., Dibenedetto, D., Cámpora Pérez, D.H.: A quantum algorithm for track reconstruction in the LHCb vertex detector (2023)
41. Pellow-Jarman, A., McFarthing, S., Sinayskiy, I., Pillay, A., Petruccione, F.: QAOA Performance in Noisy Devices: The Effect of Classical Optimizers and Ansatz Depth. arXiv:2307.10149 (2023)
42. Preskill, J.: Quantum Computing in the NISQ era and beyond. *Quantum* **2**, 79 (2018). <https://doi.org/10.22331/q-2018-08-06-79>
43. Saito, M., Calafiura, P., Gray, H., Lavrijsen, W., Linder, L., Okumura, Y., Sawada, R., Smith, A., Tanaka, J., Terashi, K.: Quantum annealing algorithms for track pattern recognition. *EPJ Web Conf.* **245**, 10006 (2020). <https://doi.org/10.1051/epjconf/202024510006>
44. Schwägerl, T., Issever, C., Jansen, K., Khoo, T.J., Kühn, S., Tüysüz, C., Weber, H.: Particle track reconstruction with noisy intermediate-scale quantum computers. arXiv:2303.13249 (2023)
45. Zhou, L., Wang, S.T., Choi, S., Pichler, H., Lukin, M.D.: Quantum approximate optimization algorithm: Performance, mechanism, and implementation on near-term devices. *Phys. Rev. X* **10**, 021067 (2020). <https://doi.org/10.1103/PhysRevX.10.021067>
46. Zhu, C., Byrd, R.H., Lu, P., Nocedal, J.: Algorithm 778: L-BFGS-B: Fortran subroutines for large-scale bound-constrained optimization. *ACM Transactions on Mathematical Software* **23**(4), 550–560 (1997)
47. Zlokapa, A., Anand, A., Vlimant, J.R., Duarte, J.M., Job, J., Lidar, D., Spiropulu, M.: Charged particle tracking with quantum annealing-inspired optimization. *Quantum Machine Intelligence* **3**, 27 (2021). <https://doi.org/10.1007/s42484-021-00054-w>